

Sliding Mode Control Strategy for Solar Charging of High Energy Lithium Batteries

Asma Mlayah^{*†}, Adel Khedher^{**}

* Electrical engineering department, National Engineering School of Sfax
LATIS- Laboratory of Advanced Technology and Intelligent Systems, Sousse University, 4002
Sousse, Tunisia

** Industrial Electronics engineering department, National Engineering School of Sousse
LATIS- Laboratory of Advanced Technology and Intelligent Systems, Sousse University, 4002
Sousse, Tunisia

(assoum.mlayah@live.fr, Adel_kheder@yahoo.fr)

†
Corresponding author; Asma Mlayah; ENISo BP 264, 4023, Sousse, Tel: +216 96 542 250
assoum.mlayah@live.fr

Received: 23.05.2018 Accepted:09.07.2018

Abstract- Lithium-Ion (Li-Ion) batteries have been widely used in electric vehicle (EV) and several other applications for their lightness and high performance. However, they imply a strict charging procedure. When a photovoltaic (PV) energy source is used, the charging task becomes more sensitive and necessitates a robust control strategy. In fact, the photovoltaic generator (PVG) is a highly nonlinear current source and depends on climatic variations.

In this paper, a sliding mode control (SMC) strategy for solar charging of a high energy Li-Ion battery is presented. The control scheme is based on a cascaded control of a current fed (CF) synchronous Buck converter powered with a PVG. It allows both maximum power point tracking (MPPT) and output voltage or current regulation of the converter.

The regulation is principally done by using the PV voltage as a control parameter. A charging algorithm providing the suitable PV reference voltage to the SM controller was proposed. Study and stability analysis of the proposed SMC were also included. The main feature of the proposed SMC is to include the PV reference voltage information in both the sliding surface, and in the equivalent control expression using the integral function. The validity of the control strategy was demonstrated through simulations under different irradiation levels in both MPPT and constant current-constant voltage (CC-CV) charging modes.

Keywords Sliding mode control; Photovoltaic generator; PV voltage control; Lithium-Ion battery; MPPT; CC-CV charging.

1. Introduction

During recent years, Li-Ion batteries have been widely used in electric vehicle (EV) and several other applications for many reasons. In turn, they are characterized with their high power and energy densities, extended lifetime and absence of memory effect [1]. In [2 and 3], the most substantial task in a battery charging system is the charging operation. When a photovoltaic (PV) energy source is used, the charging task becomes more sensitive and necessitates a robust control strategy against climatic variations [4-7].

In the PV-standalone chargers, there are several possible structures depending on the possible alternative sources included [8]. When the PV generator (PVG) is the primary

source, it is convenient to incorporate a DC Buck converter as an interface between the PV arrays and the battery. It is important to notice that the PVG has not to be analyzed as a voltage source, [9 and 14]. In fact, despite its constant current-constant voltage (CC-CV) behavior, the PVG is considered as a power limited non linear current source. It implies that the battery has to be interfaced with a voltage controlled instead of a current controlled converter since the PV current is uncontrollable.

In practice, it is evident that inserting an input capacitor to a voltage fed (VF) converter changes it to a CF one, but it has been lately demonstrated in [9] that this action alters totally the converter properties and requires the inversion of the

switching control. Hence, the ideal duty cycle expression relating the input and the output voltages of the Buck converter will imply a conventional negative instead of a positive feedback when the input voltage is the controlled variable.

In literature, several control types for DC-DC converters have been studied [10]. A widely used technique consists of directly controlling the duty cycle based on MPPT algorithms. The disadvantage of this approach is the increase of switching stress and losses. A more efficient control technique consists of integrating linear PI controllers, [9], [11-13]. However, it is limited to a special operating point. Sliding mode control SMC has been used in many researches in order to control output voltage or current of a Buck converter powered by a constant voltage source, [15- 17].

In the most works related to the SMC of the PVG, the sliding surface is generally the difference between the PV voltage and the reference [18-20]. However, when the sliding surface is derived, the reference information will be lost. Then, the voltage control cannot be applied to achieve control objectives. When the reference is the MPP voltage, this issue can be solved by exploring MPPT algorithms like in [21-24]. However, operating at the MPP is not recommended for all battery types. In [25], the sliding surface was defined by a linear combination of the PVG voltage and current, but it is also limited to MPP operation.

In this paper, we propose the design of a novel SM controller for PV voltage regulation in order to ensure solar charging of a high energy Li-Ion battery. The control scheme was inspired from a constant frequency SMC, applied previously in output voltage regulation of a Positive Output Elementary Luo (POEL) converter [26].

The novelties of the work are:

- Designing a SM control loop allowing both MPPT and output voltage or current regulation,
- Including the reference information of the SMC in both the sliding surface, and in the equivalent control expression,
- Proposing a PV charging algorithm that provides the suitable PV voltage reference for SM controller.
- Proving the reaching and existence conditions of the SMC, based on switching control inversion imposed by the CF transformation.

The paper is organized in five sections. The section 2 gives an overview of the charging system as well as control purpose and system dynamics. Control scheme of the battery charge is included in section 3. It firstly introduces the Li-Ion technology charging procedure, secondly gives the PV charging algorithm and finally details the SMC of the PV voltage. Simulation results are included in section 4. We finish this work by some conclusions.

2. Overview of the Charging System

The charging system is illustrated in Fig.1. It is composed of a PV generator, a synchronous Buck converter, a Li-Ion battery and a charge controller.

2.1. Control purpose

The Buck converter aims to adapt the PV voltage to the desired battery voltage or current. This operation is achieved by controlling the switching state through The SM controller. The charge control algorithm provides the suitable PV reference voltage to the controller. Satisfying the battery power demand is then, the main control purpose.

2.2. System dynamics

Equivalent circuit of the charging system is given in fig.2. The PVG and the battery dynamics are described by the following average state equations:

$$i_{pv} = r_s^{-1} v_{pv} \tag{1}$$

$$v_{bat} = E_o + i_o R_l \tag{2}$$

Where: r_s and R_l are respectively equivalent source and load resistances,

i_{pv} and V_{pv} are average PV current and voltage,

V_{bat} and E_0 are respectively average and rated battery voltages,

i_o is the average output current of the Buck converter.

The converter is composed of an input capacitor C_1 , two NPN Mosfets S_1 and S_2 , an inductor L and an output capacitor C_2 .

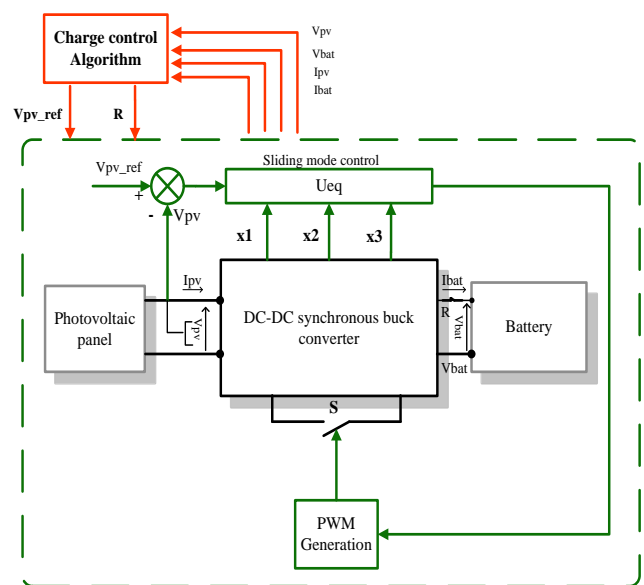


Fig. 1: Bloc diagram of the charging system.

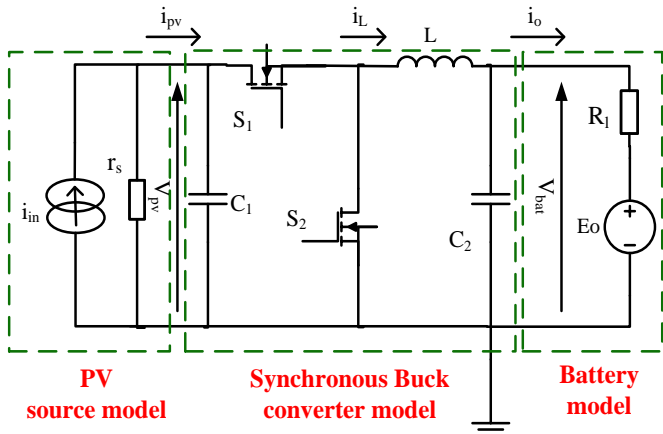


Fig.2: Equivalent circuit of the charging system.

A switching cycle depends on the ‘ON/OFF’ state of the switch S_1 . Accordingly, dynamics of the converter are presented in the following average state equations system:

$$\begin{cases} \frac{dv_{pv}}{dt} = \frac{1}{C_1}(i_{pv} - Di_L) \\ \frac{di_L}{dt} = \frac{1}{L}(Dv_{pv} - v_{bat}) \\ \frac{dv_{bat}}{dt} = \frac{1}{C_2}(i_L - i_o) \end{cases} \quad (3)$$

Where D is the duty cycle of the converter and i_L is the average inductor current.

3. Control Scheme of the Battery Charge

3.1. Control scheme of Lithium battery charging

The batteries are considered as one of the most critical components in a photovoltaic system especially when it is the case of a Li-Ion battery. In fact these batteries lifetime is extended if they are charged with respect to CC-CV charging procedure. The voltage and current charging characteristic curves are illustrated in fig.3.

The charging process is divided into three different regions:
 Region1: a pre-charge operation, it is procured by injecting a constant trickle current to the battery until the battery voltage (V_{bat}) reaches a reference pre-charge value (V_{prech}).

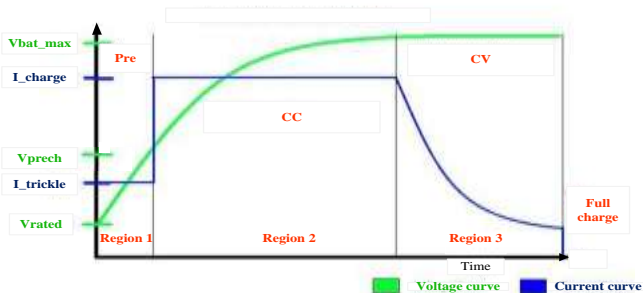


Fig.3: Li-Ion battery charge characteristics

It is generally preferred when the battery is deeply discharged and sometimes required for some Lithium battery technologies.

Region2: a constant current charge operation is suggested until V_{bat} reaches its maximum allowed value V_{bat_max} , at this moment the charge operation switches from the CC to CV.

Region3: constant voltage charging operation. In this region, V_{bat} has to be controlled until battery current (I_{bat}) shoots down to the end of charge current (I_{min}).

Using this concept, the maximum current (I_{bat_max}) will be updated during a charging cycle following the flowchart given in fig.4.

3.2. PV charging control algorithm

In order to provide photovoltaic charging of the battery, a robust control strategy is proposed. The flowchart presented in fig.5 describes the adopted control scheme.

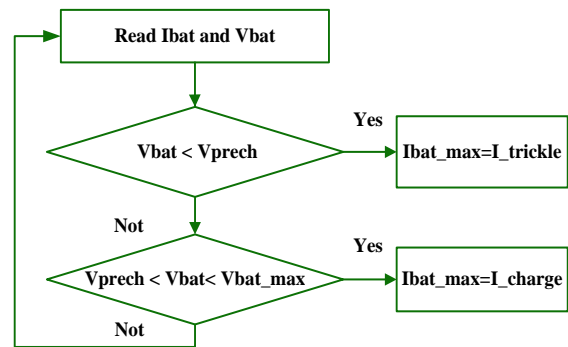


Fig.4: Lithium battery current charging flowchart

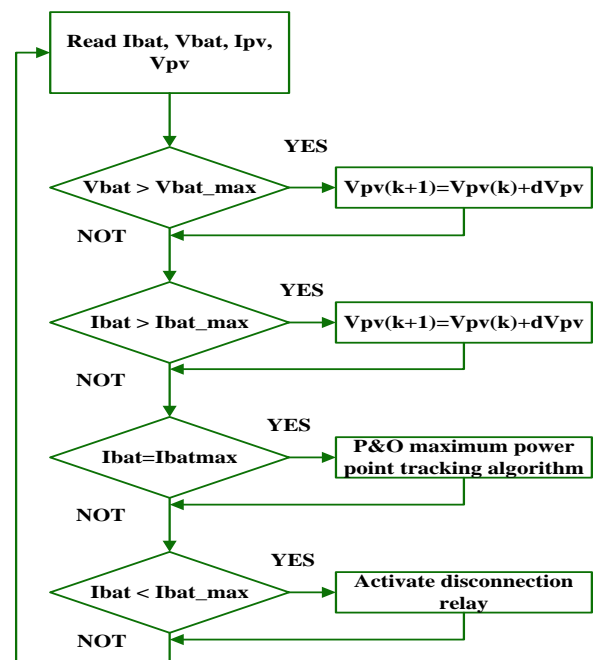


Fig.5: flowchart of control strategy proposed for the photovoltaic battery charger.

The battery current and voltage regulation consider the output voltage of the PVG as a control parameter. The MPPT algorithm used is the “Perturb and Observe” (P&O) algorithm[27] [19].

For battery current regulation, a decrease in the converter output current is obtained from PV reference voltage increments. The MPPT algorithm procures the inverse operation. If the PVG is not able to provide the desired current, or in the end of charge, a disconnection relay is used.

For battery voltage regulation, the same principle is followed. The limitation of the battery input voltage is provided by PV reference voltage increments. The inverse operation is not required. Once the PV reference voltage value is obtained, the duty cycle is directly adjusted using the SM controller, which will be detailed in the next part.

3.3. Sliding mode control of the PV voltage

SMC is based on the sliding surface S, which forces the system to stay on. In the SMC of DC converters, two implementation methods are commonly used based on the nature of the switching frequency. In the case of a variable switching frequency, a hysteresis is incorporated.

In case of a constant switching frequency (CSF), the control output is compared with a saw tooth auxiliary signal. Our study concerns CSFSMC of a Buck converter to ensure PV voltage regulation.

3.3.1. Introduction to the SMC

Considering a Variable Structure System (VSS) described by:

$$\dot{X} = A(x, t) + B(x, t)U(t) \quad (4)$$

Where U is the control vector, A and B are input and controlled matrices.

As in [26][18], a sliding surface S is expressed by

$$S(x, t) = C^T X + \psi = 0 \quad (5)$$

C is the vector containing sliding equation coefficients and ψ is a reference value.

VSS follows the switching law given by:

$$U = \begin{cases} U^+ & \text{if } S < 0 \\ U^- & \text{if } S > 0 \end{cases} \quad (6)$$

Stability of the SMC is principally analyzed by checking the existence and reaching conditions.

Existence condition is given by:

$$x(t) \in \{x / S(x) = 0\} \quad (7)$$

Reaching condition can be checked if, from any starting operating point, the SMC satisfies

$$S(x)\dot{S}(x) < 0 \quad (8)$$

The equivalent control (U_{eq}) is deduced from the invariance condition as follows:

$$\begin{cases} S(x, t) = 0 \\ \dot{S}(x, t) = C^T \dot{X} + \dot{\psi} = 0 \end{cases} \quad (9)$$

Combining (4) and (9) gives:

$$U_{eq} = -[CB]^{-1}CA(x, t) \quad (10)$$

As demonstrated in Eq.(10), the reference information is lost. This makes the system uncontrollable with the direct use of U_{eq} expression.

In the most works related to PV voltage regulation, the sliding surface is given by:

$$S(x, t) = v_{pv} - V_{ref} = 0 \quad (11)$$

Or by

$$S(x, t) = \frac{dp_{pv}}{dv_{pv}} = 0 \quad (12)$$

In Eq.(11), U_{eq} expression is given by:

$$U_{eq} = \frac{v_{pv}}{r_s i_L} \quad (13)$$

From the controller view, there is no information about the reference and the control objective will not be attended. Even when switching control function (U_n), expressed by Eq.(14) is used, a variable reference information like MPP will be always unknown from the voltage controller view.

$$U_n = -K \cdot \text{sign}(S) \quad (14)$$

In Eq.(12), the “Incremental Conductance” algorithm is explored. However, it provides only MPPT, which is not suitable for all battery types.

3.3.2. Proposed SMC

In order to include the reference information in U_{eq} expression, the reference part is replaced with a function of an order greater than one. In this case, the derivative will maintain the reference value which facilitates the implementation of the SMC.

By considering the state vector X given by:

$$X = [v_{pv} \ i_L \ v_{bat}]^T \quad (15)$$

The VSS model is described by:

$$\dot{X} = A(x, t) + B(x, t)U(t) + H \quad (16)$$

Where

$$A(x, t) = \begin{bmatrix} \frac{1}{r_s C_1} x_1 \\ -\frac{1}{L} x_3 \\ \frac{1}{C_2} x_2 - \frac{1}{R_l} x_3 \end{bmatrix}, B(x, t) = \begin{bmatrix} -\frac{1}{C_1} x_2 \\ \frac{1}{L} x_1 \\ 0 \end{bmatrix},$$

$$U(t) = \begin{bmatrix} 0 \\ U \\ 0 \end{bmatrix}^T, H = \begin{bmatrix} 0 \\ 0 \\ \frac{E_0}{R_l C_2} \end{bmatrix}$$

A, B and C are respectively state, controlled and control vectors; H is a vector describing the battery characteristics.

The proposed sliding equation is given by:

$$S_1 = \mu i_L + \int v_{pv} - V_{ref} = 0 \tag{17}$$

Equivalent control U_{eq} is expressed by:

$$U_{eq} = \frac{v_{bat}}{v_{pv}} - \frac{L(v_{pv} - V_{ref})}{\mu v_{pv}} \tag{18}$$

This expression will be used to generate the converter driving pulses.

Switching law definition and stability analysis are included in the next parts.

3.3.3. Switching law definition

In our study, the pulse width U_{eq} is the SMC output. The general discrete switching law for a Buck converter is given by:

$$U = \begin{cases} 1 & v_{pv} - V_{ref} > 0 \\ 0 & v_{pv} - V_{ref} < 0 \end{cases} \tag{19}$$

With the proposed SMC, during PWM, the switch position will be governed by the discrete switch law presented by:

$$U_s = \begin{cases} 1 & \text{if } S_1 > 0 \\ 0 & \text{if } S_1 < 0 \end{cases} \tag{20}$$

For this purpose, μ has to be chosen so that Eq.(20) would be guaranteed.

When $U_s=1$:

$$-\mu i_L < 0 < \int v_{pv} - V_{ref} \tag{21}$$

So every positive value of μ can satisfy Eq.(20).

When $U_s=0$, μ must satisfy:

$$\mu < \frac{\left| \int v_{pv} - V_{ref} \right|}{i_L} \tag{22}$$

During steady state, the current margins are defined by:

$$\begin{cases} I_L = I_{charge} & \text{in CC} \\ I_L \geq I_{trickle} & \text{in CV or in precharge} \end{cases}$$

The maximum voltage error is assumed to be $\epsilon_{max} = |v_{pv} - V_{ref}| = V_{oc}$. For a sampling period (T_e):

$$\mu < \min\left(\frac{\epsilon_{max} T_e}{2I_{charge}}, \frac{\epsilon_{max} T_e}{2I_{trickle}}\right) \tag{23}$$

By ensuring Eq.(23), the switching law will be defined.

The control scheme inversion imposed by CF transformation leads to

$$\bar{U}_s = \begin{cases} 0 & \text{if } S_1 > 0 \\ 1 & \text{if } S_1 < 0 \end{cases} \tag{24}$$

3.3.4. Stability analysis of the SMC

► Existence condition

In order to prove existence condition of the SMC, the value of U_{eq} must be limited to the following inequality:

$$0 \leq U_{eq} \leq 1 \tag{25}$$

By replacing U_{eq} with its expression in Eq.(16), we obtain:

$$\frac{\mu}{L} ((\bar{U}_s - 1) \int v_{pv}) \leq S_1 \leq \mu (i_L + \frac{1}{L} \int v_{bat}) \tag{26}$$

If the inversion of the switches control is taken into account,

$\bar{U}_s = 1 - U_s$ and Eq.(26) becomes:

$$-U_s (\frac{\mu}{L} \int v_{pv}) \leq S_1 \leq \mu (i_L + \frac{1}{L} \int v_{bat}) \tag{27}$$

Hence, every positive value of μ can satisfy the existence condition.

► Reaching condition

By considering (8), reaching condition will be met as follows:

If $\bar{U}_s = 0$, then $S_1 < 0$ and $(v_{pv} - V_{ref}) < 0$, so

$$\dot{S}_1 = -\frac{\mu}{L} v_{bat} + (v_{pv} - V_{ref}) \tag{28}$$

In order to obtain $\dot{S}_1 < 0$, the constant μ must fulfill the next condition:

$$\mu > \frac{|\mathcal{E}_{min}| L}{E_0} \tag{29}$$

Where \mathcal{E}_{min} is the minimum allowed value of $(v_{pv} - V_{ref})$.

If $\bar{U}_s = 1$, then $S_1 > 0$ and $(v_{pv} - V_{ref}) > 0$, so:

$$\dot{S}_1 = \frac{\mu}{L} (v_{pv} - v_{bat}) + (v_{pv} - V_{ref}) \tag{30}$$

To obtain $\dot{S}_1 > 0$, μ has to meet the following condition:

$$\mu > \frac{|\mathcal{E}_{min}| L}{V_{OC} - E_0} \tag{31}$$

Finally, μ must satisfy:

$$\mu > \max\left(\frac{|\varepsilon_{\min}|L}{V_{oc} - E_0}, \frac{|\varepsilon_{\min}|L}{E_0}\right) \quad (32)$$

Ensuring Eq.(23) and Eq.(32) will guarantee the stability of the SMC.

The performance comparison of the literature works and the proposed SMC is included in the tab.1.

efficiency attains 99% in irradiation less than 1000wm² and is around 95% for higher levels.

Tab.1: Performance comparison of the literature works and the proposed SMC equations

Sliding equation	Related works	Reference information	Maximum power point tracking	CC-CV regulation
$S = v_{pv} - V_{ref} = 0$	[18-20]	Constant and will be lost after derivation.	yes	not
$S = \frac{dp_{pv}}{dv_{pv}} = 0$	[21-24]	No reference information.	yes	not
$S = ai_L - bv_{pv} + ref = 0$	[25]	A constant and dimension-less reference part.	yes	not
$S = \mu i_L + \int v_{pv} - V_{ref} = 0$	Proposed sliding mode controller	Dynamic reference that will be kept in the equivalent control expression.	yes	yes

4. Simulation Results

The Control strategy was tested in both MPPT and CC-CV regulation modes. The simulations were effectuated within a sampling period $T_e=10\mu s$ and a converter switching period $T_s= 50\mu s$. The battery was initially charged to 8%. By considering Eq.(23) and Eq.(32), the SM coefficient used in simulation was $\mu=2.3e-5$. The simulink model of the charging system is presented in fig.6.

4.1. Simulation in MPPT mode

The MPPT algorithm used in this model is the P&O algorithm. Simulation parameters are included in tab.2. The irradiation profile used for this test is presented in Fig.7. Duty cycle variations are presented in fig.8. It shows that the controller tracks effectively the MPP. Its value is comprised between ‘0’ and ‘1’; this proves the stability of the SM controller. The PV voltage versus the reference voltage variations are shown in fig.9. The reference values are lower than those of the controlled variable. This is explained by to the use of the negative voltage feedback implied by the switching control inversion. A very short time response $t=15ms$ is also ensured as it is zoomed out in this figure.9. PV power characteristics are included in fig. 10. It shows the high tracking capability and the robustness under climatic variations. The efficiency of the SM controller was evaluated by the PV power transfer ratio. As shown in fig11, the

Tab.2: Simulation parameters

Characteristics of the PVG under standard conditions	
Parameter	Value
Maximum power current $I_{mpp}(A)$	8.02
Maximum power voltage $V_{mpp}(V)$	35.5
Short circuit current $I_{sc}(A)$	8.51
Open circuit voltage $V_{oc}(V)$	43.6
Maximum power $P_{max}(W)$	270
Number of cells in series	72
Design characteristics of the converter	
Parameter	Value
Input capacitor $C_1 (F)$	100 μ
Output capacitor $C_2(F)$	1.6m
Inductor L (H)	6m
Switchers S_1 and S_2	2 NPN Mosfets
Switching Frequency $f_s(Hz)$	20000
Lithium-Ion battery module specifications	
Parameter	Value
Type of cells	Li-FeS ₂
Nominal voltage (V)	1.2*N _s
Series cells number N _s	23
Parallel cells number N _p	10
Rated capacity (Ah)	1.5*N _p
Initial state of charge (%)	8
Maximum capacity (Ah)	16.154
Fully charged voltage (V)	32.51

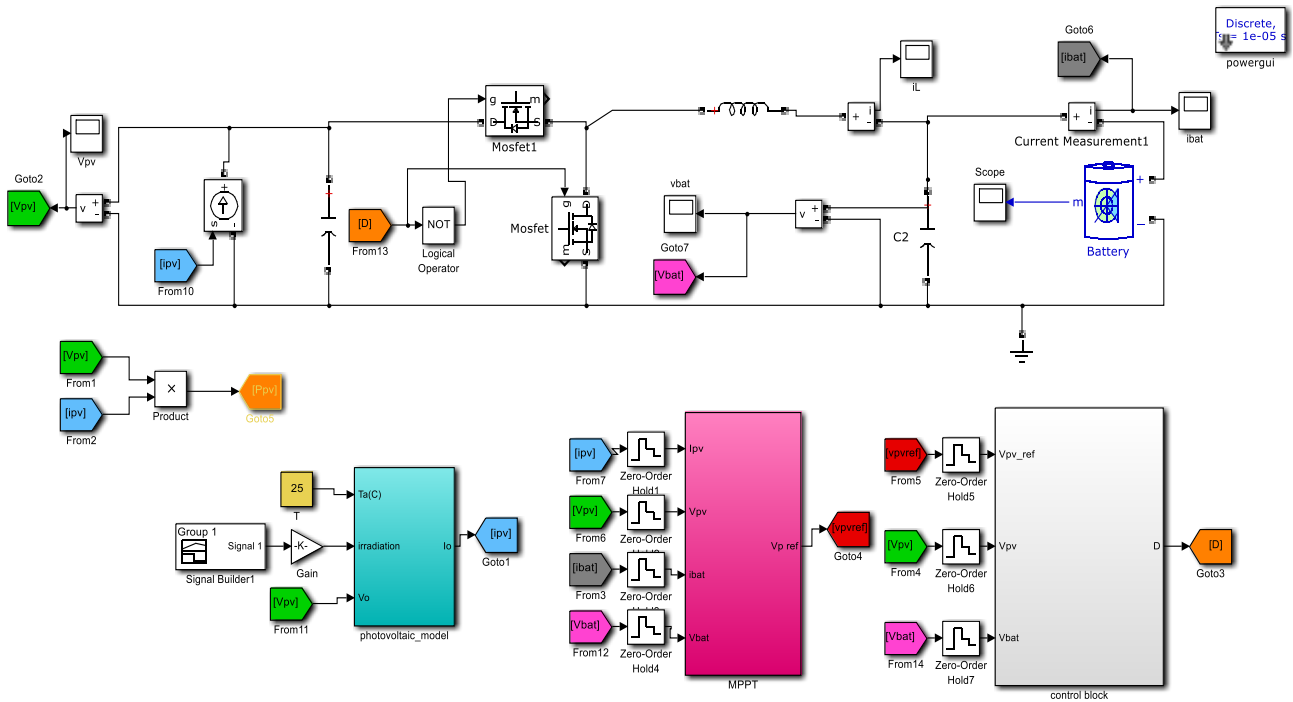


Fig. 6: Simulink model of the charging system

4.2. Simulation in CC-CV charging modes

In order to show up the different charging modes, the maximum battery voltage was set to 30V.

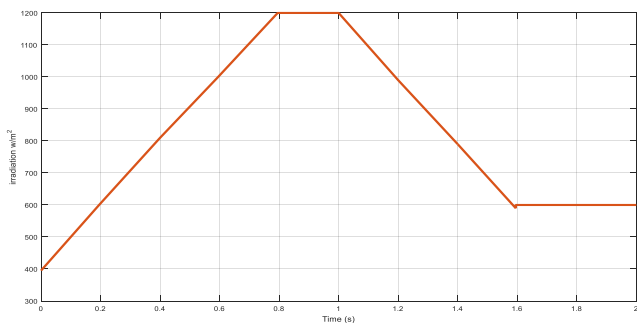


Fig.7: Irradiation profile used in MPPT test

The test was achieved during a $T_{charge}=1000s$ charging period. Simulation was done according to the irradiation profile included in fig.12. It was chosen so that the PVG satisfies the power needed.

As shown in fig.13, negative battery current is occurred. When the converter is connected to the system, the output capacitor C_2 is charged up by the battery. The negative sign is explained by the current flow from the battery to C_2 . Simultaneously, battery voltage increases from zero to its rated value as illustrated in fig.15. After the capacitor is charged up, the converter begins operating and the battery current and voltage become stabilized. The CC charge operation is shown in fig.13. The battery is firstly pre-charged with a trickle current of 0.6A until V_{bat} reaches 27.6V as illustrated in fig.14.

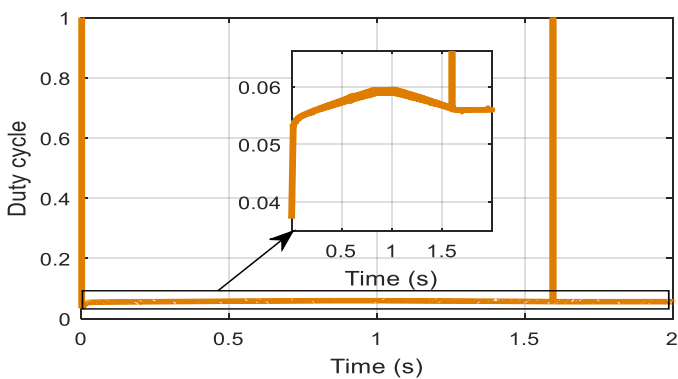


Fig.8: Duty cycle variations during MPPT

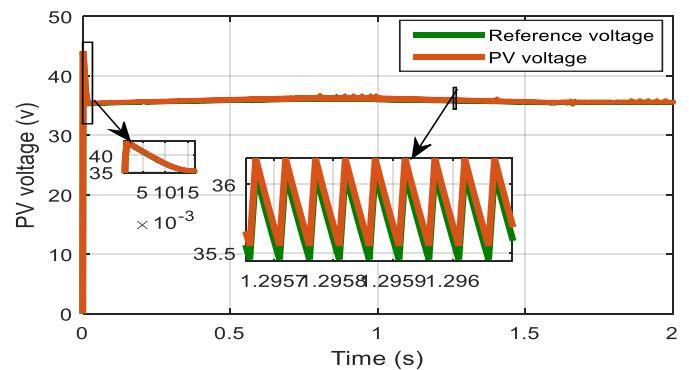


Fig.9: PV voltage versus reference voltage During MPPT

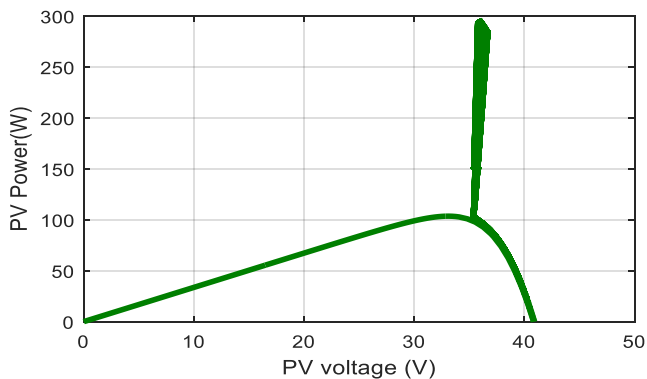


Fig.10: PV power variation during MPPT

Secondly, it is charged with a fast current of 6A until V_{bat} reaches 30V. Thirdly, the charge switches from CC to CV stage like shown in fig.15. At the end of charge, battery current drops from 6A to less than 2A. The charging operation was not completely terminated due to limited processor load memory, but this period was enough to show all regulation modes and prove the effectiveness of the control algorithm. State of charge variations are also included in fig.17.

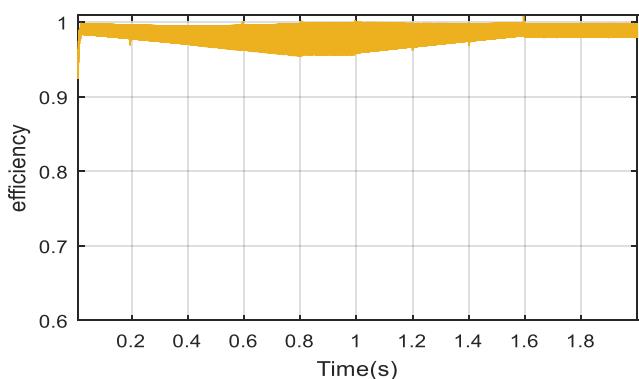


Fig.11: Efficiency of the SMC

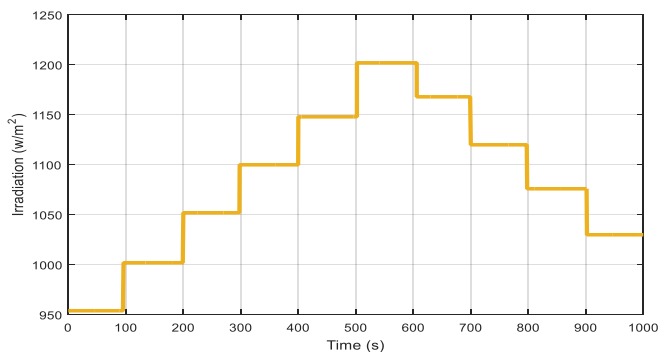


Fig.12: Irradiation profile used for CC-CV regulation

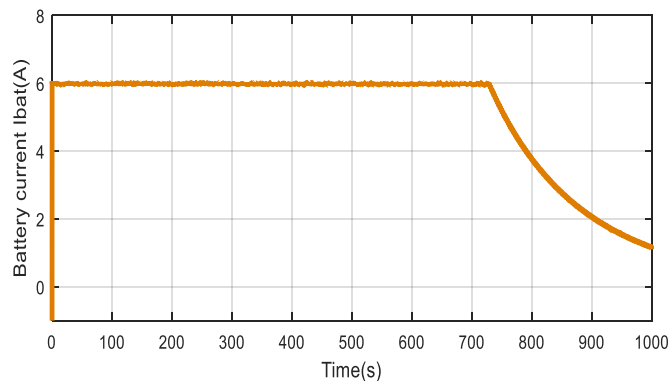


Fig.13: battery current characteristics during the charging period

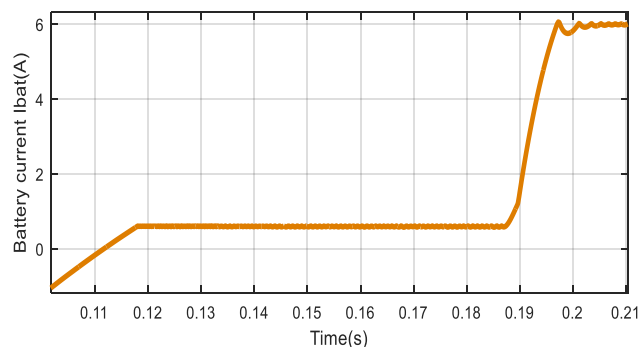


Fig.14: battery current characteristics during the pre-charge operation

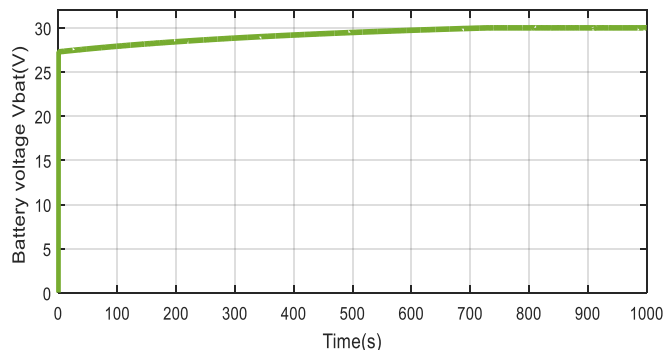


Fig.15: battery voltage characteristics during the charging period

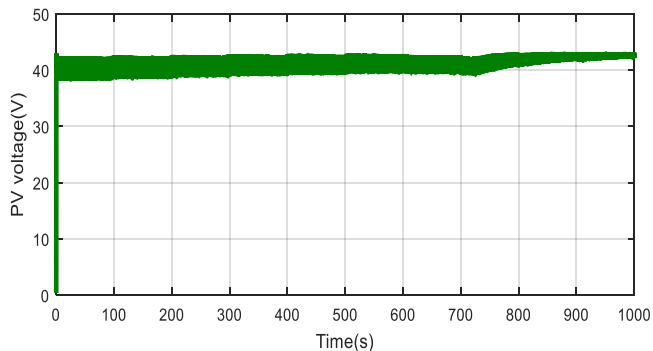


Fig.16: PV voltage characteristics during the charging period

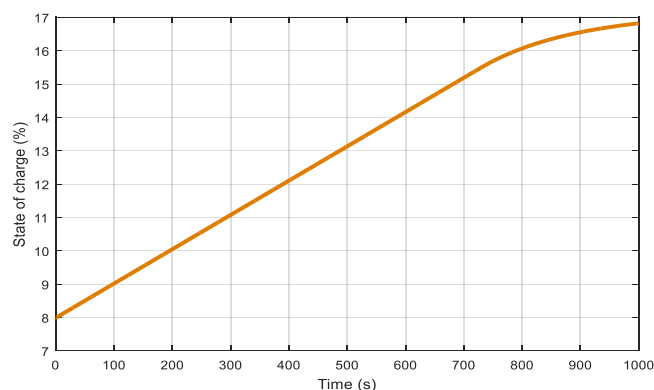


Fig.17: SOC characteristics during the charging period

5. Conclusion

In this paper, a SMC control strategy for Li-Ion battery charging using PV energy has been introduced. Theoretical analysis of the proposed sliding surface equation has been developed in order to design the charge controller. The main feature of this SMC is including the reference voltage information in the control expression. A charging algorithm has been proposed in order to provide the suitable reference value. Simulation results under MPPT and CC-CV regulation modes confirm the effectiveness of the control strategy proposed in this paper.

6. References

- [1] I. Baccouche, S. Jemmali, A. Mlayah, B. Manai, N. Essoukri Ben Amara, "Implementation of an improved Coulomb-counting algorithm based on a piecewise SOC-OCV relationship for SOC estimation of Li-Ion battery", *International Journal of Renewable Energy Research IJRER*, Vol.8, No.1, March, 2018.
- [2] BUCHMANN, Isidor. Battery university. CADEX Electronics Inc..[Online] Available at: <http://batteryuniversity.com> [Accessed April 2018], 2018.
- [3] T. Sakagami, Y. Shimizu, H. Kitano, "Exchangeable batteries for micro EV's and renewable energy", 6th International Confernece on Renewable Energy Reasearch and Application ICRERA, USA, Nov 5-8, 2017.
- [4] M. Chiandone, C. Tam, R. Campaner, G.Sulligoi, "Electrical storage in distribution grids with renewable energy sources" ", 6th International Confernece on Renewable Energy Reasearch and Application ICRERA, USA, Nov 5-8, 2017.
- [5] A. Weiss, H. Ziegerhofer, "High safety photovoltaic insolar power supply systems employing re-used Lithium-Ion cells", 5th International Confernece on Renewable Energy Reasearch and Application ICRERA, UK, Nov 20-23, 2016.
- [6] M. Longo, W. Yaïci, F. Fioadelli, "Electric vehicles charged with residential's roof solar photovoltaic system", 6th International Confernece on Renewable Energy Reasearch and Application ICRERA, USA, Nov 5-8, 2017.
- [7] S. Hattori, H. Eto, F. Kurokawa, "High power density battery charger for plug-in Micro EV", *International Journal of Renewable Energy Research IJRER*, Vol.8, No.2, June 2018.
- [8] B.M.H. Jassim, H.M. Jassim, "Modelling of a solar array simulator based on multiple DC-DC converters", *International Journal of Renewable Energy Research IJRER*, Vol.8, No.2, June 2018.
- [9] M. Sitbon, J. Leppäaho, T. Suntio, A. Kuperman, "Dynamics of photovoltaic-generator-interfacing voltage-controlled Buck power stage", *IEEE Journal of Photovoltaics*, Volume: 5, Issue: 2, Pages: 633 – 640, 2015.
- [10] M. KH. Al Nassiri, R. Bayindir, E. Hossain, "Fuzzy logic controller for DC-DC Buck converter with constant power load", 6th International Confernece on Renewable Energy Reasearch and Application ICRERA, USA, Nov 5-8, 2017.
- [11] Z. Mokrani, D. Rekioua, T. Rekioua, "Modelling, control and power management of hybrid photovoltaic fuel cells with battery bank supplying electric vehicle", *International Journaal of Hydrogen energy* Issue: 39, Pages: 15178-15187, 2014.
- [12] M. G. Villalva, T. G. De Siqueira, E.Ruppert, "Voltage regulation of photovoltaic arrays: small-signal analysis and control design", *IET Power Electronics*, Volume: 3, Issue: 6, Pages: 869 – 880, 2010.
- [13] M. Chakib, A. Essadiki, T. Nasser, "A comparative study of PI, RST, and ADRC control strategies of a doubly fed induction generator based wind energy conversion system", *International Journal of Renewable Energy Research IJRER*, Vol.8, No.2, June 2018.
- [14] L. Nousiainen, J. Puukko, A. Mäki, T. Meso, J. Huusari, J. Jokipii, J. Viinamäki, D. Torres Lobera, S. Valkeakahti, T. Suntio, "Photovoltaic generator as an input source for power electronic converters", *IEEE Transactions on Power Electronics*, Volume: 28, Issue: 6, Pages: 3028-3038, 2013.
- [15] V. Utkin, "Sliding mode control of DC/DC Converters", *Journal of Franklin Institue* Issue: 350, Pages: 2146-2165, 2013.
- [16] E. Vidal-Idiatre, A. Marcos-Pastor, R. Giral, J. Calvente, L. Martinez-Salemero, "Direct digital design of a sliding mode based control of a PWM synchronous Buck converter", *IET Power Electronics*, Volume:10, Issue:13, Pages: 1714-1720, 2017.

- [17] H. Guldemir, "Study of sliding mode control of DC-DC Buck converter", *Energy and Power Engineering*, Issue:3, Pages: 401-406, 2011.
- [18] I. S. Kim, M. B. Kim, M. J. Youn, "New maximum power point tracker using sliding-mode observer for estimation of solar array current in the grid-connected photovoltaic system", *IEEE Transactions on Industrial Electronics*, Volume: 53, Issue: 4, Pages: 1027 – 1035, 2006.
- [19] O. Boukli-Hacene, A. chermitti "Robust regulation of the photovoltaic voltage using sliding mode control as part of a MPPT algorithm" , *International Journal of Computer Applications* , Volume 78 – No.11,pages : 0975 – 8887, September 2013.
- [20] A. Jimenez Brea, I. Ortiz-Rivera, A. Salazar-Llinas, J. Gonzalez-Llorente, "Simple photovoltaic solar cell dynamic sliding mode controlled maximum power point tracker for battery charging applications", *Applied Power Electronics Conference and Exposition (APEC)*, 2010.
- [21] P. Huyong and B. Cho, "Design and analysis of a microprocessor controlled peak-power tracking system", *IEEE Transactions on Aerospace and Electronic Systems*, 32(1), Pages:182-189, 1996.
- [22] A. Belkaid, I. Çolak, K. Kayisli, "Optimum control strategy based on an equivalent sliding mode for solar systems with battery storage", 2016 *IEEE International Power Electronics and Motion Control Conference (PEMC)*, Pages: 1262 – 1268, 2016.
- [23] J. Ghazanfari, M. Farsangi, "Maximum power point tracking using sliding mode control for photovoltaic Array", *Iranian Journal of Electrical & Electronic Engineering*, Vol. 9, No. 3, pages : 189-196, Sep. 2013.
- [24] H. Battista, R.J .Mantz, "Variable structure control of a photovoltaic energy converter", *IEEE Proceeding-Control theory and Applications*. Vol: 149, No4, July 2002.
- [25] Y. Levron, D. Shmilovitz, "Maximum power point tracking employing sliding mode control", *IEEE Transactions On Circuits and Systems*, Vol:60, Issue: 3, March 2013.
- [26] Y. He, F. L. Luo, "Sliding-mode control for dc-dc converters with constant switching frequency", *IEE Proceedings - Control Theory and Applications*, Volume: 153, Issue: 1, Pages: 37 – 45, 2006.
- [27] M. ben Smida, A. sakli, "A comparative study of different MPPT methods for grid-connected partially shaded photovoltaic systems", *International Journal of Renewable Energy Reaserch IJRER*, Vol:6, Issue: 3, July 2016.